Omni: Volumetric Sensing and Actuation of Passive Magnetic Tools for Dynamic Haptic Feedback

Thomas Langerak*, Juan José Zárate*, David Lindlbauer, Christian Holz, Otmar Hilliges
Department of Computer Science, ETH Zurich, Switzerland

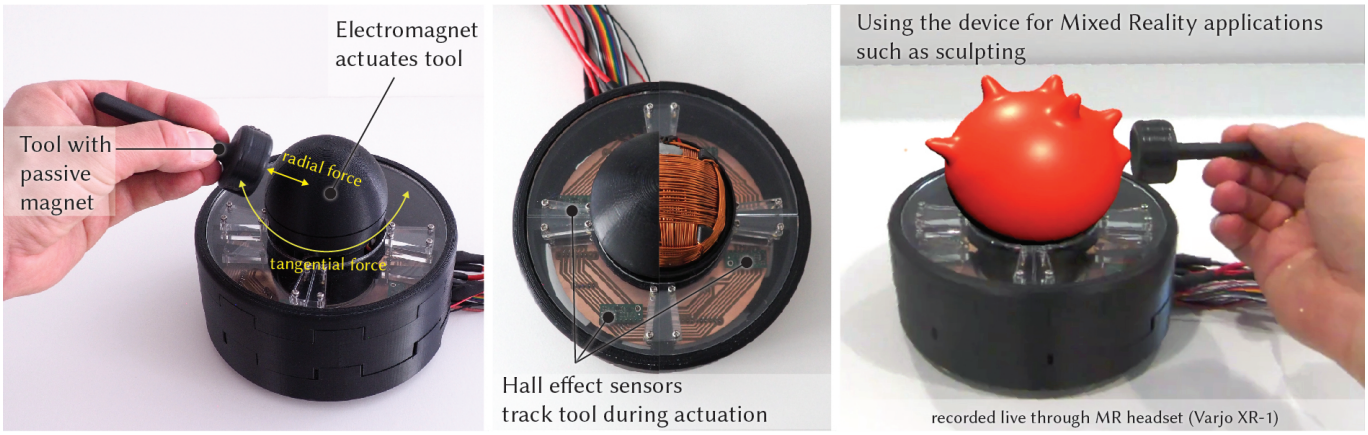

Figure 1. We present Omni, a device that can simultaneously actuate and sense the position of a passive handheld tool. This is enabled through integrated hall effect sensors and our novel gradient-based optimization scheme. Omni can for example be used in 3D applications such as MR sculpting.

ABSTRACT

We present Omni, a self-contained 3D haptic feedback system that is capable of *sensing* and *actuating* an untethered, passive tool containing only a small embedded permanent magnet. Omni enriches AR, VR and desktop applications by providing an active haptic experience using a simple apparatus centered around an electromagnetic base. The spatial haptic capabilities of Omni are enabled by a novel gradient-based method to reconstruct the 3D position of the permanent magnet in midair using the measurements from eight off-the-shelf hall sensors that are integrated into the base. Omni's 3 DoF spherical electromagnet *simultaneously* exerts dynamic and precise radial and tangential forces in a volumetric space around the device. Since our system is fully integrated, contains no moving parts and requires no external tracking, it is easy and affordable to fabricate. We describe Omni's hardware implementation, our 3D reconstruction algorithm, and evaluate the tracking and actuation performance in depth. Finally, we demonstrate its capabilities via a set of interactive usage scenarios.

*Authors contributed equally.

UIST'20, October 20–23, 2020, Minneapolis, MN, USA

ISBN 978-1-4503-6708-0/20/04…$15.00

DOI: https://doi.org/10.1145/3313831.XXXXXXX

Author Keywords

Haptic feedback; Electromagnetic sensing; Electromagnets; Mixed Reality

CCS Concepts

•Hardware → Haptic devices; •Human-centered computing → Mixed / augmented reality; Haptic devices;

INTRODUCTION

Emerging computing paradigms, such as Virtual and Augmented Reality, promise an immersive digital experience. Existing VR and AR systems have first and foremost been focused on high-fidelity visual and auditory displays to render coherent spatial experiences to users. However, to increase the immersion into a carefully crafted artificial world, it is necessary to also support the sense of touch and to provide tactile feedback when interacting with virtual objects in 3D.

To overcome the lack of physical interaction with the virtual world, VR controllers are commonly augmented with vibro-tactile actuators (e. g., hand-held [41, 24] or worn on the palms [55]). Typical actuators are eccentric rotating mass motors (e. g., ERM vibration motors in Xbox controllers [39]) or smaller linear resonant actuators (e. g., Sony DualSense). Such actuators are limited to rendering of vibrotactile stimuli that emanate from the whole controller. Hence, rendering of precisely localizable spatial feedback is difficult to impossible.

In this paper, we explore an alternative strategy to rendering precisely controllable haptic feedback for spatial applications such as AR/VR. Forgoing active actuators in a handheld controller, our approach relies on electromagnetism to actuate an

otherwise passive tool with embedded (ferro-)magnetic material. This configuration allows delivery of up to 2 N of radial and tangential forces in midair without the requirement for a rigid attachment or anchoring of the tool to the environment.

One of the core challenges in enabling high-fidelity free-space haptic interactions is to reliably track the input device in space and to *simultaneously* exert forces. While optical tracking systems can be used for 3D localization, they require significant instrumentation of the user's environment and thus are impractical for real deployments.

Embracing this challenge, we propose an integrated system that can locate the tool in free-space and deliver finely controllable haptic feedback all via the same modality. Our system, dubbed *Omni*, consists of an omnidirectional spherical electromagnet that delivers attractive and repulsive forces in radial and tangential directions onto a small, handheld magnet (see Figure 1). To track the tool's location, we leverage eight integrated hall sensors, positioned in two separate XY-planes with respect to the electromagnet's coils such that the sensor readings allow for the reconstruction of the tool's position based on the distortion of the magnetic-field caused by the tool's motion. Compared to approaches that rely on passive magnets only [4, 36] , our setting is significantly more challenging due to the use of an active electromagnet. Here, the electromagnetic actuation and the sensing interfere since two physical phenomena (e. g., tool motion and electromagnet control) create a single, super-imposed magnetic field.

To decompose the resulting superposition of magnetic fields, we introduce a novel 3D positioning algorithm. Our formulation reconstructs the magnet's 3D position by minimizing the residual between the predicted magnetic field strength at a given location and the actual measurement picked up by the Hall sensors. The formulation is amenable to gradient-based optimization and we show that the problem can be solved via a quasi-newton solver in real-time and that it achieves an accuracy of 6.9 mm after a one-shot calibration procedure.

We demonstrate the capabilities of our approach through a series of interactive use-cases, some shown in Figure 11, that leverage the ability to track the handheld tool in 3D and while simultaneously delivering dynamically adjustable haptic feedback to it. The magnet fits inside passive tools, such as the 3D-printed stylus that supports fine-grained interaction tasks and can alternatively serve as a joystick. We showcase applications in gaming, accessibility, mixed reality, and 3D CAD design that make use of *Omni's* 3D tracking and 3D actuation.

We detail our software and hardware implementation and then thoroughly assess *Omni's* sensing and actuation capabilities. We find that *Omni* can continuously deliver up to 0.6 N in any direction when in the vicinity of the sphere, and the electromagnetic coils are heating up to a sustainable 47 ^{o}C. The peak force of our system tops out at 1.8 N for repelling and -3.1 N for attractive forces to the sphere; and ± 2 N in the tangential plane to the sphere. *Omni* can actuate the magnet at 100Hz and sense and estimate its 3D position at 40Hz.

Contributions

In summary, we make the following contributions in this paper:

- A fully self-contained system, combining actuation and tracking components,
- a novel algorithm for the reconstruction of the 3D tool position under electromagnetic actuation,
- a thorough technical evaluation of algorithm, yielding an accuracy of 5 mm without actuation and 7 mm with the electromagnet on,
- assessment of the force generation capabilities, showing up to 2 N of haptic force in any direction,
- an exploration of use cases afforded by *Omni*.

Our method can be extended to any apparatus involving a permanent magnet, integrating spatial position reconstruction and spatial actuation into a single apparatus. Our software implementation and hardware designs are available as open source at https://ait.ethz.ch/projects/2020/omni/.

RELATED WORK

Haptic technologies have found a renewed interest in the human-computer interaction community due to the recent reemergence of Augmented and Virtual Reality systems. *Omni* is related to research that have proposed novel actuation, systems that render haptic feedback without contact, as well as electromagnetic sensing and tracking.

Mechanical haptic feedback

The most common form of rendering haptic feedback have been vibrotactile actuators. They are popular in commercial devices, such as the controllers of game consoles, AR and VR controllers, and mobile phones. They can also be embedded directly into displays [59] or in clothing [18, 40].

Vibrotactile actuators usually produce coarse and global feedback, especially when used in handheld controllers (e. g., rendering touch contact in VR [5, 16]). Researchers have investigated how to overcome this limitation, such as by rendering interpolations between several such motors [26] or strategically distributing them across a controller (e. g., placing them under the fingers to render local grasp feedback [34]).

Alternatives to vibrotactile feedback often involve more complex articulated haptic elements, such as arms and braking mechanisms (e. g., [37, 51, 56, 3, 66, 50]). In general, these types of systems can provide local haptic feedback at higher levels of fidelity and can render both, tactile and kinesthetic feedback. Further extensions of such systems are exoskeletons [19, 15], gloves [17, 22], and tilt-platforms [45, 30]. These platforms are usually (rigidly) anchored and can therefore supply large forces. These approaches, except DextrES [22], rely on mechanical structures and anchoring the environment. Therefore, their use is mostly limited to high-end applications such as teleoperation.

Contact-free haptic feedback

A second line of research focuses on contact-free haptics, which provide rich and strong feedback, and overcome the need for expensive and complex mechanical setups [13]. Within the contact-free domain, many different actuation devices have been explored, e. g., ultra-sound pressure waves [23], active control of stylus motions [29] and drones [21].

The most popular and practical actuators in this domain use magnetism. The simplest form of magnetism is delivered by passive magnets that are embedded into interactive objects (e. g., [60]). The recent advance of consumer 3D printing has allowed this approach to actuate objects with arbitrary shape and function [65, 42]. A big shortcoming of passive magnets, however, is the lack of dynamic control over them and thus the forces users perceive during interaction.

Electromagnetic haptic feedback

The shortcoming of passive magnets can be addressed using electromagnetism and computational control of magnetic forces. Two-dimensional arrays of electromagnets can be combined with passive magnets that are worn [58, 63, 60, 2, 8, 6, 9] or embedded in tools and interactive objects [28, 43, 57]. The actuation area can be increased by attaching an electromagnet to a biaxial linear stage [32, 33]. Similarly, by leveraging the electromagnetic forces in a coil between two permanent magnets, large and grounded forces can be delivered onto a joystick [7]. The main drawback of this approach is the requirement for a mechanical connection, limiting the range-of-motion and impeding contact-free haptics.

Senkal et al. [48, 49] and Li et al. [35] propose to use magnetorheological fluids in joysticks. With the help of an electromagnet field the internal friction can be significantly increased. This allows for a large breaking force, however it does not allow to add energy to the system.

Perhaps the most well-known haptic interface that builds on Lorentz forces is the Butterfly Haptics Maglev [10, 11]. The design of this system consists of a flotor bowl with six integrated coils to which an interaction handle is rigidly. This flotor bowl is levitated between magnets assemblies that are part of a stator bowl. Due to the Lorentz levitation, haptic feedback can be achieved in a degree of rotary movement and also a small translation. Due to the small movements allowed, the device is mainly suitable for small-scale manipulations, e. g., where only the fingers are used. The design of our system is fundamentally different. We use a single omnidirectional electromagnet, thereby largely increasing the rotary capabilities. Furthermore, by omitting the levitating flotor bowl our device greatly reduces the complexity and therefore makes it easier to fabricate, thereby more likely to foster adaptation. Finally, our design allows for contact-free haptics; which is not possible in the Butterfly system.

Closely related work also includes Omnimagnet by Petruska et al. [44] and its variants [25]. Similar to *Omni*, their system generates an omnidirectional magnetic field. Their design differs by using three nested cuboid-shaped coils, causing force decay as the user moves along the surface of the device as well as an obstruction of heat dissipation. This limits the maximal strength and duration of actuation [1], and also makes the device only suitable for rendering vibrotactile stimuli [64]. Due to the cuboid shape, the center-to-center distance between the electromagnet and the permanent magnet is not constant among the surface, which causes high variance in the forces perceived. In contrast, *Omni*'s design is spherical, symmetrical, and has intertwined coils. This results in better heat dissipation and less variance in the force, thereby arguably improving the user experience.

Omni's actuator builds on our previous work on spherical electromagnets that can render haptic sensations [62]. However, *Omni*'s design differs significantly in multiple aspects and *Omni's* capabilities improve the haptic actuation capabilities by a large margin (force of 2 N for *Omni* vs. 1 N for [62]). First, the electromagnetic design of *Omni* as well as the choice of permanent magnet were determined through a COMSOL optimization that yields significant improvements in terms of force generation capabilities. In practice, this means that with a similar form factor, *Omni* can deliver forces that are *over 2 times stronger* while developing less heat, which is critical in operation. *Omni* also integrates 3D tracking through the same modality into its base, whereas our earlier work does not provide any sensing capabilities and relies entirely on external, vision-based system to track the tool. Finally, in the present work, we provide real-world results in terms of force delivery strength and accuracy, and explore interactive scenarios.

Magnetic tracking

Permanent magnets have been used for tracking objects in 3D, ranging from styli and other interactive objects [36, 31], jewelry [4] all the way to fingers [20], joints, and other biological tissues [12, 52]. Ample research exists on tracking permanent magnets. Most of the existing literature uses isotropic (i. e., spherically) shaped permanent magnets, because the dipole model most accurately resembles these [27]. However, some work also uses electromagnets attached to fingertips [14]. Due to this the fingers can be tracked individual.

One of the biggest challenges is that a closed-form solution of the magnet states (e. g., position) is unlikely to exist in most scenarios. Therefore optimization-based methods are commonly used [47, 53] and more recently also neural networks [46]. However, these methods were often employed offline, suffered from large latency, or converged to local minima.

A key related work is Magnetips by McIntosh et al. [38]. They use a permanent magnet attached to a fingertip to interact with a watch. The permanent magnet is tracked around the watch and also used to provide vibrotactile haptic feedback. Magnetips multiplexes actuation and sensing. However, this causes significant delays (2 ms for every swap between tracking and actuating). Which may pose an issue for scenarios that require continuous interactions.

The work that most resembles our work from an algorithmic point of view is [53]. They track multiple spherical magnets online using an analytical Jacobian allowing solving with a quasi-newton method. In contrast, *Omni* tracks a single magnet while compensating for drastically changing electromagnetic fields, rather than tracking multiple permanent magnets in a static environment. We do this by adjusting the dipole model so that it is suitable for electromagnetism. We also propose a novel formulation of the position reconstruction problem and a implementation in PyTorch that can leverage the frameworks auto-grad capabilities, thus avoiding the need for an analytical Jacobian.

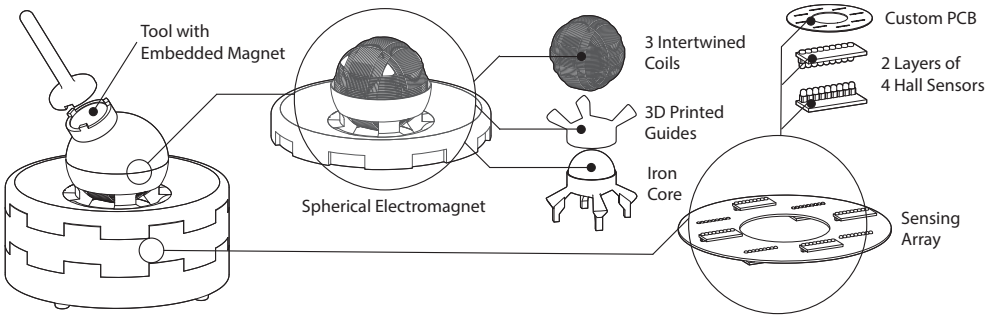

Figure 2. Overview of our system. A 3D printed base contains the 3 DoF intertwined coils and the circular PCB with an array of eight hall sensors. Arbitrarily shapes tools can be 3D printed and augmented with a permanent magnet, to interact with *Omni*.

SYSTEM OVERVIEW

Omni is a self-contained haptic feedback system that simultaneously integrates 3D tracking and actuation using the same modality (see Figure 2). Through actuating an untethered, contact-free tool by means of a magnetic field, our device supports rendering precise haptic attractive and repulsive forces as well as accurate tracking without the need for any external infrastructure or markers. Our system allows for rich interactions with and haptic perception of dynamic virtual surfaces.

Our goal is to enrich AR/VR and other 3D applications via *Omni* and a minimally instrumented tool. Simplicity of the haptic prop, and a walk-up-and-use experience were important design goals of our work. Furthermore, to create rich immersive experiences, such a system must be able to deliver different types of high-fidelity haptic forces and precisely sense user input without the requirement for any external tracking. Moreover, we aim for a self-contained device that is affordable and easy to manufacture.

The actuation mechanism used in *Omni* is based on the working-principle proposed in [62]. We build up an hemispherical shell base whose core houses a symmetric omnidirectional electromagnetic actuator. Three interwoven and mutually orthogonal coils generate the haptic forces. By controlling the current in each coil, we can precisely configure the exerted force onto an external magnet, such as the one inside the 3D stylus tool. As the tool approaches the sphere, *Omni* is able to provide independently controlled radial and tangential forces. Our design contributes several important improvements over [62] that allow us to provide twice the amount of force (2 N in either direction) and for much longer periods without suffering from self (over-)heating. Although the tool is contact-free, the haptic force that the user perceives has its reaction force on the support base. In this sense, the user perceives a grounded forces even if there is no mechanical link to the base. In our current implementation, *Omni* rests on a surface (e. g., table), though it is compact and could be mounted on a robotic end effector to deliver large-scale 3D feedback. This would allow for haptic feedback in a large volume, which would be beneficial for VR applications. In this case, however, geomagnetism should be taken into account more strongly.

Beyond the improved actuator, our main contribution lies in the integration of the *Omni* actuator with a fully self-contained real-time tracking method of the tool. To this end, eight Hall sensors are distributed below the interactive sphere. Each sensor reads a combination of the magnetic field generated by the tool, super-imposed by the electromagnetic field generated by the actuator. We use a gradient-based optimization method to locate the magnet's 3D position based on the hall sensors' readings, running at an interactive rate of 40 Hz.

ELECTROMAGNETIC TRACKING AND ACTUATION

To support interactive experiences, our actuator needs to dynamically adjust its output according to the desired haptic feedback at a given time and tool position. We now describe our real-time approach to reconstruct the tool's 3D position given the readings observed by the Hall sensors, and the control strategy to govern the electromagnet-tool interaction.

Dipole-dipole model

We build on prior work in approximate models of magnetic fields for simulation purposes [54, 62] to model the magnetic field in real-time. Such approximate models require only the magnitude, orientation, and position of each dipole magnet. We make similar assumptions here. It is important to note that, by placing the sensors low in the hardware base, we ensure a large-enough distance from the sensor to both, the electromagnet and the tool magnet and thus avoid early saturation. The dipole assumption allows for efficient computation of the magnetic field at the sensor locations,

$$\mathbf{B}(\mathbf{r},\mathbf{m}) = \frac{\mu_0}{4\pi}\frac{3\,\hat{\mathbf{r}}\,(\hat{\mathbf{r}}\cdot\mathbf{m})-\mathbf{m}}{|\mathbf{r}|^3}\,, \tag{1}$$

where μ_0 is the relative permeability of air, $\mathbf{r}$ is the vector from the magnetic source to the position of the sensor that reads $\mathbf{B}$. $\mathbf{m}$ is the magnetic moment, $\mathbf{m_e}$ for the electromagnet or $\mathbf{m_p}$ for the permanent magnet respectively. Figure 3 illustrates the dipoles in their respective coordinate systems.

In the case of $\mathbf{m_p}$, the dipole of the tool magnet, θ and φ are the angles with regard to and around the positive z-axis, respectively (Fig. 3). The three components of the tool dipole are given by,

$$\mathbf{m_p} = \frac{1}{\mu_0} * Br * V * \begin{bmatrix}\sin(\theta)\,\cos(\varphi)\\ \sin(\theta)\,\sin(\varphi)\\ \cos(\theta)\end{bmatrix}\,, \tag{2}$$

where V is the volume of the permanent magnet and Br its remnant magnetic flux, i. e., its permanent magnetization in

Tesla units. The electromagnet operates far from saturation, allowing us to write its magnetic dipole $\mathbf{m_e}$ as being proportional to the actuation current:

$$\mathbf{m_e} = \mathbb{C} * \mathbf{I}^T \ , \tag{3}$$

where $\mathbf{I} \in \mathbb{R}^3$ is a vector containing the electrical current supplied to each coil, and $\mathbb{C} \in \mathbb{R}^{3\times3}$ is a calibration matrix, obtained via measuring $\mathbf{m_e}$ at different known currents. Note that for coils that are completely orthogonal and thus align perfectly with the sensor axis, $\mathbf{C}$ is a diagonal matrix. In our implementation, we found that the elements outside the diagonal are around 1.5% the diagonal elements in magnitude.

To compute the magnetic field at each $i-$sensor location via Eq. 1, the super-imposition of the different magnetic field sources, namely of the permanent magnet $\mathbf{B_p}$, the electromagnet $\mathbf{B_e}$, and background noise $\mathbf{B_n}$, needs to be considered:

$$\mathbf{B_i} = \underbrace{\mathbf{B}(\mathbf{r_{s_i}} - \mathbf{r_p}, \mathbf{m_p})}_{\mathbf{B_p}} + \underbrace{\mathbf{B}(\mathbf{r_{s_i}}, \mathbf{m_e})}_{\mathbf{B_e}} + \mathbf{B_n} \ . \tag{4}$$

3D position estimation

At the core of creating dynamic interactive experiences lies the ability to react in real-time to the movement of the user. Thus a method to acquire the tool position with sufficient accuracy and precision with low latency is required.

This is challenging due to the dynamic super-imposition of the various magnetic fields (see Eq. 4). More precisely, directly computing the tool's position from the sensor readings would require inversion of Eq. 1, which is non-linear and hence non-invertible, rendering an analytical solution for the tool position infeasible. To overcome this difficulty, we introduce a reconstruction algorithm that optimizes an estimate of the tool's position given the Hall sensor readings in real time.

We propose an iterative model fitting approach for 3D position estimation. We minimize the residual between the *expected* sensor reading $\mathbf{B_i}$, as predicted by our model of the magnetic field (Eq. 4) given the current actuation, and the *actual* measurements acquired by the Hall sensors $\tilde{\mathbf{B}}_\mathbf{i}$. In this setting, the optimization variables are the tool's 3D position and its orientation. With a good initialization, which we attain by careful construction of the hardware, and exploiting the redundancy in the measurements, this algorithm provides accurate estimates of the tool's position in 3D, with a mean accuracy of 6.9±3.2 mm, as shown in our technical evaluation.

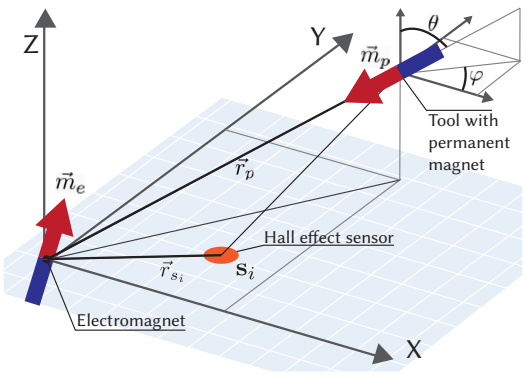

Figure 3. Omni's coordinate system with electromagnet, tool with permanent magnet and example of a hall effect sensor.

For each Hall sensor ($\mathbf{s_i} \in \mathbf{S}$) defined by its 3D coordinate, $\mathbf{s_i} = [s_x, s_y, s_z]^T$, we seek to find the tool position $\mathbf{r_p} = [p_x, p_y, p_z]^T$ and orientation $\mathbf{o} = [\theta, \varphi]^T$ that provides the best model fit to the current reading. We use the global coordinate system for the sensors position $\mathbf{r_{s_i}}$ and tool position $\mathbf{r_p}$ with an origin in the center of the electromagnet, i. e., $\mathbf{r_e} = [0,0,0]$. The optimization problem is then given by:

$$\arg\min_{\mathbf{r_p},\ \mathbf{o}} \Bigg[\sum_{\mathbf{s_i}\in\mathbf{S}} \sum_{x,y,z} \mathbf{w_i} \Big(\mathbf{B_p}(\mathbf{r_{s_i}} - \mathbf{r_p}, \mathbf{m_p}) + \mathbf{B_e}(\mathbf{r_{s_i}}, \mathbf{m_e}) + \mathbf{B_n} - \tilde{\mathbf{B}}_\mathbf{i} \Big)^2 \Bigg] \ , \tag{5}$$

where $\mathbf{w_i}$ selectively weighs the sensor axes depending on the value it reads (i. e., a completely saturated sensor receives a weight close to 0). We pre-compute $\mathbf{B_e}$ for different actuation strengths and $\mathbf{B_n}$ denotes the background noise measured at startup. We empirically found that including the tool orientation θ and φ as free variables improves the position estimates by roughly 2 mm in euclidean distance. However, the orientation estimates were too noisy to use in interactive settings.

We minimize Eq. 5 via iterative optimization. Specifically, we use PyTorch's second-order L-BFGS optimizer, which typically works well for non-smooth optimization instances such as ours and requires no parameter tuning. Gradients are computed automatically via auto-grad.

Our method relies on known sensors locations obtained via one-shot calibration. We empirically found that an initial estimate of the sensors' locations in the range of 1 mm accuracy is required to support robust convergence of the algorithm.

Actuation

Given the 3D pen-position we can now deliver dynamically adjustable attractive and repulsive forces via the electromagnet to create a desired haptic experiences. It remains in the hand of an application designer to decide with which intensity and in what direction the tool is pulled or pushed according to the desired user experience. *Omni* is able to control 3 of the 6 Dof available, summing up forces and torques. We derive the case in which the goal is to control the three components of the haptic force $\mathbf{F_h}$, while controlling torques would follow an analogue derivation.

Under the magnetic dipole-dipole approximation, the force applied to the permanent magnet in the tool can be computed from the previous magnetic moments for the tool, $\mathbf{m_p}$, and the electromagnet magnetisation $\mathbf{m_e}$ we seek to control (see Figure 3). Using the formulation of Yung et al. [61] and rewriting it in matrix form allows us to derive a simple control law for the parameters of the electromagnet $\mathbf{m_e}^{set}$, given the location of the tool $\mathbf{r_p}$, its dipole orientation $\mathbf{m_p}$, and the desired haptic force $\mathbf{F_h}$:

$$\mathbf{m_e}^{set} = a_1 \ [\mathbb{D} + a_2 \ \mathbb{I}]^{-1} * \mathbf{F_h} \tag{6}$$

where $a_1 = \frac{4\pi r_p^5}{3\mu_0}$, $a_2 = \langle \mathbf{m_p}, \mathbf{r} \rangle$ can be computed from the tool position information (as described in the previous section). The matrix $\mathbb{D}$ has elements

$$d_{i,j} = m_{p_i}\, r_{p_j} + m_{p_j}\, r_{p_i} - 5\, a_2\, (r_{p_i}/r_p^2)\,, \tag{7}$$

where m_{p_i} and r_{p_i} denotes the $i-$component of the dipole $\mathbf{m_p}$ (Eq. 2) and position $\mathbf{r_p}$, respectively (see Figure 3). $\mathbb{I}$ is a diagonal identity matrix. Finally we use the calibration matrix from Eq. 3 to find the electrical current to be applied to the individual coils:

$$\mathbf{I}^{set} = \mathbb{C}^{-1} * \mathbf{m_e}^{set}\,. \tag{8}$$

By combining Eq. 8 and 6, the vector of desired haptic force $\mathbf{F_h}$ can be mapped into three actuation currents $\mathbf{I}^{set}$. This 3D-forces-onto-3D-currents mapping can be always decomposed into tangential and radial forces, using the tool's local coordinates system.

To only consider attractive and repelling forces and ignore the tangential component, Eq. 8 can be further simplified to:

$$\mathbf{I}^{set} = \alpha \frac{2\pi r_p^3}{3\mu_0}\, \mathbf{r_p}\,, \tag{9}$$

where α is the intensity of the force and its sign denotes attraction or repulsion relative to the sphere. In this particular case, the electrical current vector, the direction of the tool and the tool dipole can be assumed to be always co-linear.

Control implementation

The tracking algorithm, electromagnet control and user facing components (AR applications) run on a commodity gaming PC (Intel Core i7-8086K with 6 cores at 4 GHz, 32 GB RAM, NVIDIA GeForce GTX 1080 Ti) on Windows 10. The system is implemented in Python 3.7 and uses PyTorch's L-BFGS solver. The optimization-based tracking algorithms runs at 40Hz at the highest precision (6.9 mm). The AR applications were implemented in Unity 2019, SteamVR and the Varjo Unity Plugin v2.4.

Hardware integration

Our hardware design is driven by two main factors. First, through a finite element analysis (FEA), we determined the physical characteristics of our hardware, such as coil diameter, core size, as well as the parameters of the permanent magnet embedded in the hand-held tool. This reference design strikes a balance between compact form-factor and force-generation capabilities. Second, we use off-the-shelf components for sensors and the voltage controller, in-house wound coils and in-house milled printed circuit boards (PCBs) to precisely mount the sensor's boards. Reproducing *Omni* only requires readily available components and few specialized tools, if any. The main hardware components are illustrated in Figure 4.

Figure 5 plots the results from an FEA of the tool's magnet to identify the best configuration given our current spherical electromagnet design. We use a magnet with 15 mm diameter and 7 mm height (volume of 5 cm^3), which corresponds to a point in the dark red region of the plot, where the output vertical force at 5 A is maximal. Please note that these characteristics

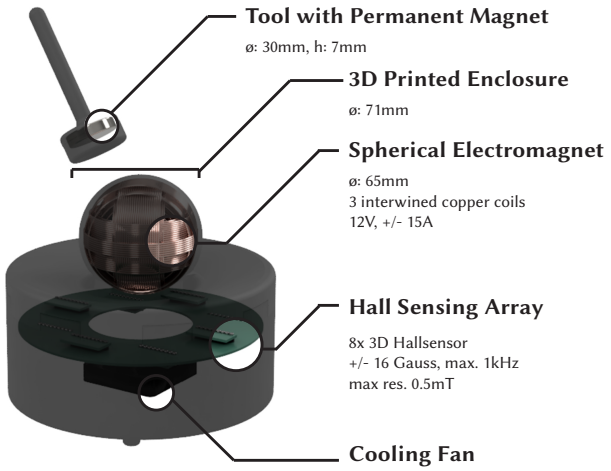

Figure 4. *Omni* hardware overview. Annotated view of the most important components of the system. All components can be acquired commercially or are easy to produce in a standard FabLab. A top-down view of the physical device can seen in Figure 1.

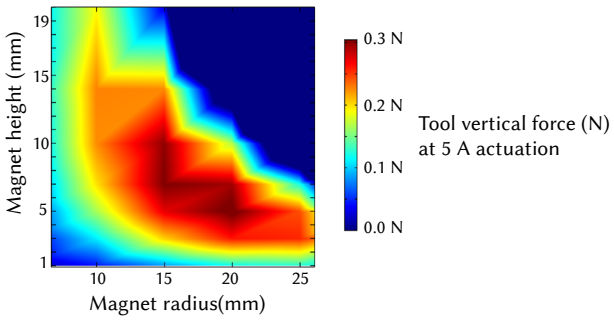

Figure 5. Finite element analysis of actuation force as function of the permanent magnet's dimensions. Our current design is based on a 15×7 mm magnet, which provides maximal force generation capabilities. However, the plot illustrates that there is a pareto-front of similarly well performing shapes that could allow for different tool designs.

hold for magnet with similar volume: either wider and shorter cylinders or narrow and tall, providing ample room for the design of the handheld prop. Importantly, a bigger magnet would not necessarily perform better and may decrease performance (top right region of the plot), since the weight of the magnet counteracts the vertical actuation in repel mode.

The omnidirectional electromagnet is based on a 30 mm diameter soft iron core encapsulated in 3D printed guides, aimed to assist during the manual winding (see Fig. 2). In contrast to [62], we construct our coils layer by layer in an interwoven fashion. We iteratively add layers of x-winding, y-winding and z-winding, respectively, until we reach an outer diameter of 65 mm. We use round copper wire with an external diameter of 0.9 mm (19 AWG) to obtain roughly 150 turns per coil. We employed a total cable length of $L_x = 21.4$ m, $L_y = 22.7$ m and $L_z = 24$ m for the x-, y- and z-coil respectively. Since the x-coil is wound first, it has an smaller radius per layer, i. e., a shorter perimeter per turn. The measured resistance of the coils are $R_x = 0.643\ \Omega$, $R_y = 0.676\ \Omega$ and $R_z = 0.708\ \Omega$. The systems supports up to 15 A of actuation current, which

translates to a power of 157 W. To help removing the Joule heating generated within the coils, we place a brushless DC fan under the sphere (*CUI Devices, 0.524 m^3/min*), and include air intakes on the side of *Omni*.

To enable accurate and reliable tracking, it is paramount that the electromagnet and the Hall sensors are mounted rigidly with respect to each other. To ensure this, we fabricated custom PCBs using a desktop PCB milling machine (*Bantam Tools*). The ring-shaped sensor PCB is located below the electromagnet, with two circular arrays that mount 4 Hall Sensors each (LIS3MDL, *Pololu*). All sensors are precisely aligned with the coil planes, such that each sensor's local coordinate system aligns with the global frame. The Hall sensors sample at up to 1kHz and are read out by a micro-controller (*Teensy 4.0*), that communicates with the host PC.

We implemented an open-loop strategy to control the generated force. The approach is based on an analytical relation between the force, the coil actuation and the tool location (Eq. 6), and relies on a few-point calibration.

For actuation we use three H-bridges (*Pololu G2 18v17*) to control the current of each coil with a pulse width modulation (PWM) of the voltage. Given Ohm's law, we can directly control the current via the voltage if the resistance of each coil is known. Since electromagnets suffer from drift due to self-heating (and thus resistance changes), our system includes a coil-resistance drift compensation implemented directly on the actuation micro-controller. Two current sensors (*INA260, Adafruit*) provide an independent measure of the voltage and current of each coil. A sliding window average of the measured current I_i and voltage V_i are used to stabilize force-generation.

TECHNICAL EVALUATION

Omni's capability of delivering convincing haptics sensations relies on the performance of two main components: tracking of the tool position and in-air actuation. We performed technical evaluations on both aspects. In summary, *Omni* is able to reconstruct the position of the tool with an accuracy of $6.9(\pm 3.2)$ mm and can deliver peak forces of up to $\pm$ 2 N, and 0.615 N continuously.

Besides this technical evaluation, we demonstrate *Omni's* interactive capabilities in the application section. We refer readers to Zarate et al. [62] for a psycho-physics evaluation of a comparable underlying actuation mechanism, showing that users can discriminating at least 25 discrete force locations.

Tracking evaluation

To evaluate *Omni*'s tracking accuracy, we compared our position estimates to those of a 10-camera Optitrack setup, capturing a tracking space of 1.2 $\times$ 0.8 m with submillimeter accuracy at 100 Hz. We configured *Omni* to run in precision mode at a frame rate of 40 Hz. For both tracking methods, we recorded the position and rotation angles. We evaluated the accuracy of *Omni* in two conditions: *no actuation* and *actuation*. In the *no actuation* condition, no current was sent to the coils. In the *actuation* condition, the coils were actuated using a sawtooth function sending current between -4 and 4 Amperes for each axis.

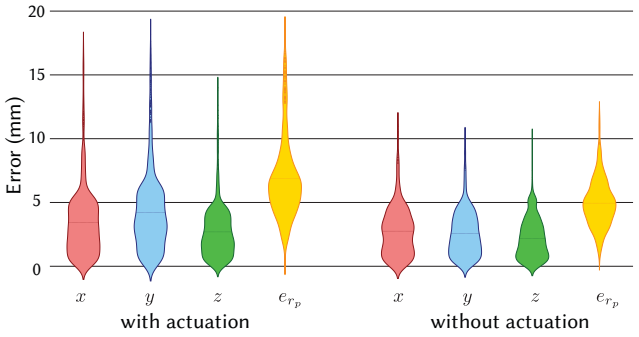

Figure 6. Distribution of tracking error with and without current applied to the electromagnet.

For each condition, the pen was moved around the center of *Omni* at a distance of up to 10 cm, covering the area around the device. We collected 1600 samples for the *no actuation* condition and 2600 samples for the *actuation* condition, both at roughly 5 Hz.

Results

We found that the average difference between the two tracking systems is $e_{r_p} = 4.9(\pm 1.8)$ mm in the *no actuation* condition and $e_{r_p} = 6.9(\pm 3.2)$ mm in the *actuation* condition. Analyzing each axis separately, we found that $\mathbf{e_{r_p}} = [3.4;\ 3.1;\ 2.7]$ mm for the tracking errors and *no actuation* and $\mathbf{e_{r_p}} = [4.4;\ 5.2;\ 3.3]$ mm in the *actuation* condition. The results are summarized in Figure 6.

Finally, we tested our formulation with and without the orientation estimation of the magnet. While we found that including these additional optimization variables improves the accuracy of the position estimates, these estimates are unstable and not yet useful for interactive applications. Intuitively it makes sense that including the orientation in the model fitting improves position estimation since the orientation of the magnet does influence the magnetic field. Furthermore, it is known that the model we leverage [61] works best for spherical magnets (e. g., point estimates of positions) and hence the models' approximation error may be a source of noise in the orientation estimates. We leave an extension of the reconstruction method to 5-DoF for future work.

Actuator evaluation

Omni's 3 DoF spherical electromagnet produces a force on the permanent magnet in the tool by dynamically adjusting the magnetic field through currents in the orthogonal coils. To quantify this actuation, we measured the radial and tangential forces on different locations around the electromagnet in *Omni*'s spherical base. We place a 3D-printed hemisphere over the electromagnet (see Figure 7). The hemisphere has three slots to place a test magnet (*S-30-07-N, Supermagnete*, same as in tool) and two force sensors (*FSAGPNXX1.5LCAC5, Honeywell*). The force sensors were attached between the electromagnet and the test magnet to measure radial force, and to the side of the test magnet to measure tangential forces.

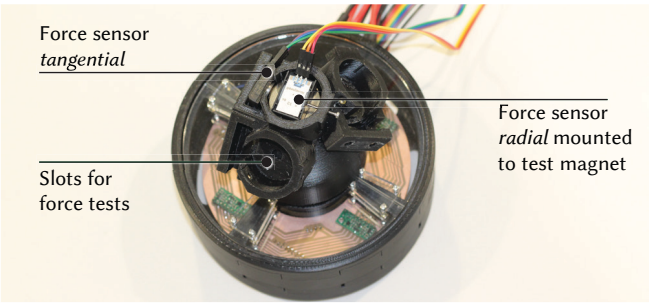

Figure 7. Setup for actuator evaluation. An additional 3D printed hemisphere is placed on top of *Omni* to hold the force sensors.

Results

We generally observed a linear response of actuation with respect to the applied current. On top of the electromagnet, we measured a maximum vertical repulsive (radial) force of 1.95 N at $I_z = 14.6$ A and a maximum attractive force of -3.04 N at $I_z = -14.6$ A, shown in Figure 8. When *Omni* applies $I_z = +3.7$ A, it compensates for the weight and snapping and the magnet starts to levitate[1]. Note that at this position, the force is the sum of the electromagnetic actuation, the snapping to the core, and the gravitational attraction. The weight of the tool produces a force of $F_r = -370$ mN (38 gr), while ferromagnetic snapping yielded additional 170 mN of force, combined these produce an attracting radial force of $F_r = -540$ mN without actuation ($I_z = 0$ A). All those components contribute to users' perception of force. On top of the sphere, the weight and snapping are orthogonal to the x-axis and y-axis and do not influence the radial forces along those axes. Consistently, we measured a linear response on those axes of the form $Fr_{x-axis} = 0.122\ [N/A]\ I_x$ and $Fr_{y-axis} = 0.142\ [N/A]\ I_y$.

For the other locations in our test setup (horizontal to vertical), we observed forces in the range of ± 2 N at ± 15 A with the corresponding corrections for weight and snapping. Note that the forces have been measured when the tool was in contact with *Omni*'s hemisphere. The force intensity decays with $1/(d_0 + g)^4$, where g is the air-gap between the tool and the sphere. The parameter $d_0 = 41$ mm is the center-to-center distance between the electromagnet and the permanent magnet when the tool touches the sphere. For example, for $g = 10$ mm, the reachable range of forces drops to ± 835 mN. At 30mm from the hull this reduces to 0.2N

Evaluation of EM heating

To test the stability of the generated forces and the thermal capabilities of our system, we ran two experiments. First, we set the $y-$axis coils to maximum actuation current $I_y = 15$ A for 25 seconds and let it cool down afterwards to test the system under *peak-force* conditions. Second, we set the same coil to 1/3 of the maximum actuation and we let it run for 15 minutes, to test under *constant-force* conditions. Figure 9 shows the evolution of the generated force and the temperature of the coil for both conditions.

[1]In this paper we use the term *levitation* in the sense of *compensate its weight completely*. A complete levitation would need to control the actuation in all the three axis to keep the magnet floating in place.

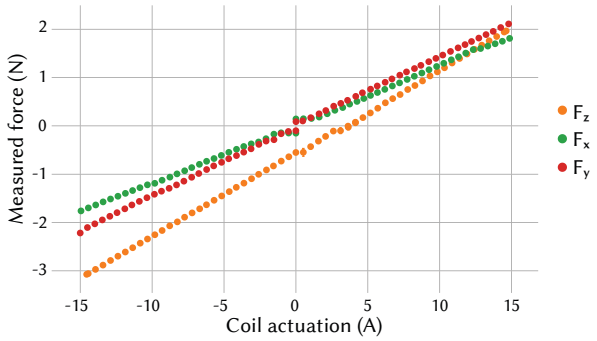

Figure 8. Radial and tangential forces on the permanent magnet as a function of coil actuation I_x, I_y and I_z, for the magnet located on top of the sphere (Fig 7). Force was collected with a compression-like force sensor.

During *peak-force*, the system delivers a force of 2.04 ± 0.04 N. Starting from room temperature (24 °C), the actuator heats up to 39 °C but only 40 seconds after the actuation has been turned off, showing the system thermal's inertia. The $\Delta T = 15$ °C during this intense actuation peak shows that our system is capable of thermally buffering and dissipating the heat generated by intense forces even during tens of seconds.

In our *constant-force* experiment (Figure 9, *bottom*), the force remained constant within the limits 0.615 ± 0.015 N and for a duration of 15 min, even when the temperature of the coils (and their resistances) significantly changed. In addition to compensating for the actuation drifts, we used the coils' resistance changes over time as the limiting factor to avoid overheating of the coils and the 3D printed parts, in case the system is required to apply maximum forces for minutes.

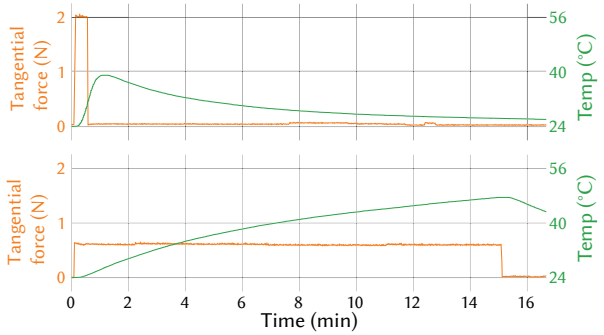

Figure 9. Temporal evolution of the self-heating of the coils for two different types of actuation. Top: a *peak-force* of 2 N ($I_y = 15$ A) during 25 seconds. Bottom: a *constant-force* of 600 mN ($I_y = 5$ A) during 15 minutes.

APPLICATIONS

We implemented a series of applications to showcase Omni's potential in supporting spatial interaction with virtual objects that is supported by strong haptic sensations as shown in Figure 11. While *Omni* can support traditional desktop interaction with haptic cues (e. g., free-form tool-based gesture input), we focus our applications on mixed and virtual reality scenarios that are inherently spatial. Specifically, we demonstrate scenarios in MR, which benefit most from *Omni*'s walk-up-and-use nature to track and haptically actuate an untethered, small

magnet in the space around *Omni*'s base. We implemented our applications using a video pass-through Mixed Reality device (Varjo XR-1), shown in Figure 10. *Videos and photos were recorded live through Varjo's software.*

Figure 10. We combine *Omni* with a video see-through MR device (Varjo XR-1) to showcase the applications.

Sculpting

Figure 11 illustrates how *Omni* haptically supports 3D sculpting and CAD design. Here, the user finely selects locations on a 3D base object for extrusion by means of the stylus, which is tracked through *Omni*. When extruding individual bumps from the starting configuration, the user can probe and feel the compliance of the material, rendered through attractive and repulsive forces. Having extruded several bumps from the original shape, the user may inspect the 3D object visually as well as haptically, as *Omni* renders collisions with the tool through tangential actuation. Following this 3D interaction scenario, *Omni*'s haptic capabilities could be scaled to common 3D editing techniques such as grid snapping, guided object rotation, and 3D transformation.

Non-rigid object exploration

Omni's tracking and actuation also lends itself for haptically rendering geometric objects that are non-rigid and may have anisotropic material properties, such as geographical surfaces, enlarged microscopic surfaces, or other complex geometries. We demonstrate how *Omni* generates haptic feedback while touching and poking a virtual dragon that is configured to simulate rubber-like material properties. Here, the force *Omni* renders increases with the amount of object deformation, which portrays the *physical behavior* more accurately than would be possible to experience through mere visual feedback.

Gaming

Finally, we demonstrate how *Omni* can be used for enhancing the experience of gameplay. Using the magnet-equipped tool as a joystick, we demonstrate how users can steer a car in an AR racing game. The combination of *Omni*'s haptic feedback and visual control over the car increases the level of immersion provided by the system, as haptic and visual sensations render a coherent experience. For example, *Omni* renders car collisions with forces whose magnitude depend on collision speeds.

DISCUSSION

Omni is capable of tracking a passive tool with an accuracy of roughly 6.9 mm and, *at the same time*, deliver a maximum force of up to 2 N to the tool. This is enabled by our novel gradient-based approach in 3D position reconstruction that accounts for the force exerted by the electromagnet. Over extended periods of time, *Omni* can comfortably produce a force of 0.615 N without the risk of overheating. In our applications, we show that *Omni* has the potential for a wide range of usage scenarios, specifically to enrich AR and VR interactions. *Omni* is, however, not limited to spatial applications. We believe that *Omni* can be a valuable addition to desktop interfaces, e. g., navigating through video editing tools or gaming. We plan to broaden *Omni's* usage scenarios in the future.

The overall tracking performance of *Omni* suffices for interactive applications such as the ones shown in this paper. The accuracy could be improved by adding more hall sensors, or optimizing their placement further (e. g., placing them on the outer hull of the device). Furthermore, a spherical tip on the passive tool that closer resembles to dipole in our magnetic model could further improve *Omni*'s accuracy. We believe, however, that the design of *Omni* represents a good balance of cost and complexity of manufacturing, and accuracy.

Our current implementation of *Omni* and the accompanying tracking and actuation algorithms assumes the presence of a single passive tool. Our method, however, potentially generalizes to tracking multiple passive tools by accounting for the presence of multiple permanent magnets. This poses another interesting challenge: the magnets of multiple tools will interact with each other, i. e., attract and repel each other. The electromagnet will also jointly interact with those tools, leading to challenges in terms of computation and convergence. We believe that our gradient-based optimization can account for such interactions and plan to investigate this in the future.

In developing and testing our applications, we found that *Omni*'s current frame rate of 40 Hz suffices for many interactive scenarios. The frame rate is a trade-off between speed and accuracy. In our tests, decreasing the desired accuracy in our optimization doubled the frame rate, while resulting in errors in the 3D position estimation of more than 1 cm, however. Finding the sweet spot for this trade off depends on the application. While our applications worked well with 40 Hz and the current accuracy, more intricate actions such as high-precision sculpting might benefit from higher frame rates *and* precision. Reducing the latency of several system components (e. g., sensor latency, convergence time) is another interesting direction of future research.

Overall, the main benefits of *Omni* lie in the high accuracy and large force it can produce. It does so without mechanically moving parts, which would be subject to wear. Such wear is not the case for our device, because it is exclusively based on electromagnetic force. We believe that different form factors of *Omni* (e. g., body-mounted, larger size) can present interesting directions of future research. A body-mounted version could be interesting for VR applications in which the user moves in 3D space. The larger size could result in more discernible points. Additionally, the influence of strength on user

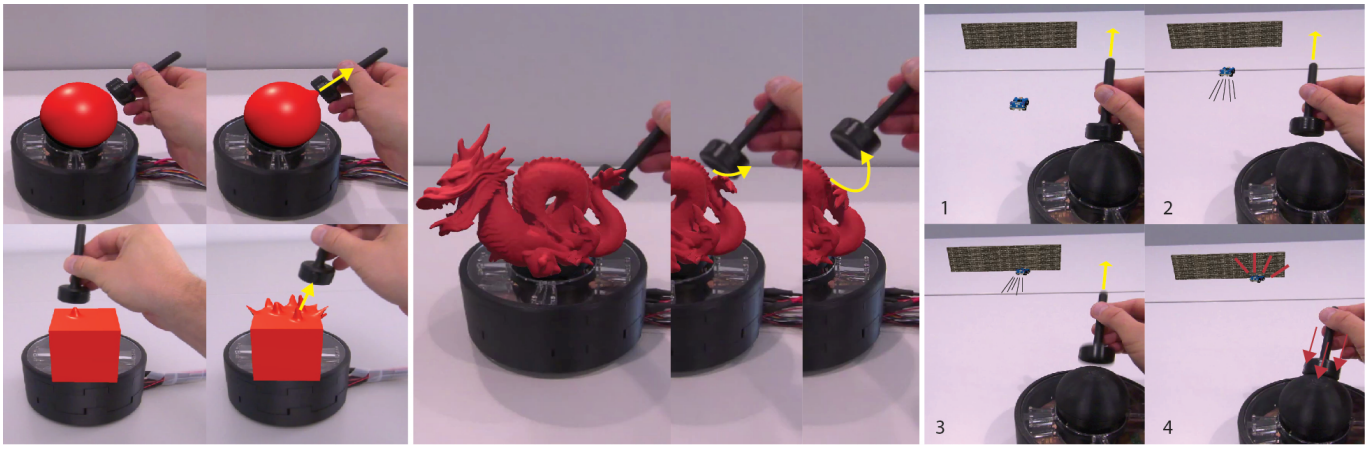

Figure 11. We present possible use cases for *Omni*. *Left* show the possibilities in 3D CAD design, in this case sculpting. *Center* shows a user is exploring and manipulating an augmented reality object. For both applications, users can feel the shape of the outer hull of the objects. *Right* shows a racing game. Once the car collides with the wall, the pen gets pushed to the base. *Arrows indicate movement and are drawn on top of the photo to increase clarity*.

perception and factors such as just-noticeable-difference will allow us to characterise the benefits and challenges of *Omni*, and electromagnetic haptic devices in general. We believe that *Omni* opens interesting direction for future research in terms of novel devices, and magnetic actuation and tracking.

CONCLUSION

We have introduced a novel electromagnetic platform that simultaneously tracks and actuates a permanent magnet in the space around it. Our self-contained base assembly *Omni* integrates 3D magnetic sensing using Hall sensors as well as magnetic actuation through radial and tangential forces produced by three orthogonal electromagnetic coils integrated into a single sphere. Our core contribution is decomposing the natural interference caused by simultaneous magnetic tracking and actuation. What enables our approach is our novel gradient-based optimization method that minimizes the difference between estimated and observed magnetic fields, thereby affording 3D tracking capabilities with a mean error of 6.9 mm during actuation forces of up to 2 N. *Omni*'s capabilities allow spatial interaction systems to integrate 3D tracking and actuation of untethered, free-ranging tools, simply by embedding a small permanent magnet. We have demonstrated a series of example applications that make use of *Omni*'s capabilities and believe that the open source release of our implementation and designs will help further advance spatial interaction research.

ACKNOWLEDGEMENTS

This work was supported in part by grants from ERC (OPTINT StG-2016-717054) and the ETH Zurich Postdoctoral Fellowship Programme (ETH/Cofund 18-1 FEL-39).

REFERENCES

[1] 2017. *A Thermal Transient Model of Heat Transfer Within an Omnimagnet*. ASME International Mechanical Engineering Congress and Exposition, Vol. Volume 8: Heat Transfer and Thermal Engineering. DOI: http://dx.doi.org/10.1115/IMECE2017-72120 V008T10A046.

[2] Alaa Adel, Mohanad Mansour, Mina M Micheal, Ahmed Abdelmawla, Islam SM Khalil, and Sarthak Misra. 2019. Magnetic Localization for an Electromagnetic-Based Haptic Interface. *IEEE Magnetics Letters* 10 (2019), 1–5. DOI: http://dx.doi.org/10.1109/LMAG.2019.2908149

[3] Bruno Araujo, Ricardo Jota, Varun Perumal, Jia Xian Yao, Karan Singh, and Daniel Wigdor. 2016. Snake Charmer: Physically Enabling Virtual Objects. In *Proceedings of the TEI '16: Tenth International Conference on Tangible, Embedded, and Embodied Interaction (TEI '16)*. ACM, New York, NY, USA, 218–226. DOI: http://dx.doi.org/10.1145/2839462.2839484

[4] Daniel Ashbrook, Patrick Baudisch, and Sean White. 2011. Nenya: Subtle and Eyes-Free Mobile Input with a Magnetically-Tracked Finger Ring. In *Proceedings of the SIGCHI Conference on Human Factors in Computing Systems (CHI '11)*. Association for Computing Machinery, New York, NY, USA, 2043–2046. DOI: http://dx.doi.org/10.1145/1978942.1979238

[5] Hrvoje Benko, Christian Holz, Mike Sinclair, and Eyal Ofek. 2016. NormalTouch and TextureTouch: High-fidelity 3D Haptic Shape Rendering on Handheld Virtual Reality Controllers. In *Proceedings of the 29th Annual Symposium on User Interface Software and Technology (UIST '16)*. ACM, New York, NY, USA, 717–728. DOI: http://dx.doi.org/10.1145/2984511.2984526

[6] Peter Berkelman, Sebastian Bozlee, and Muneaki Miyasaka. 2013. Interactive rigid-body dynamics and deformable surface simulations with co-located maglev haptic and 3D graphic display. (2013).

[7] Peter Berkelman and Michael Dzadovsky. 2009. c. In *World Haptics 2009-Third Joint EuroHaptics conference and Symposium on Haptic Interfaces for Virtual Environment and Teleoperator Systems*. IEEE, 517–522. DOI:http://dx.doi.org/10.1109/WHC.2009.4810897

[8] Peter Berkelman, Muneaki Miyasaka, and Juaquin Anderson. 2012. Co-located 3D graphic and haptic display using electromagnetic levitation. In *2012 IEEE Haptics Symposium (HAPTICS)*. IEEE, 77–81. DOI: http://dx.doi.org/10.1109/HAPTIC.2012.6183773

[9] Peter Berkelman, Bernadette Tix, and Hamza Abdul-Ghani. 2018. Electromagnetic position sensing and force feedback for a magnetic stylus with an interactive display. *IEEE Magnetics Letters* 10 (2018), 1–5. DOI:http://dx.doi.org/10.1109/LMAG.2018.2886339

[10] Peter J Berkelman, Zack J Butler, and Ralph L Hollis. 1996. Design of a hemispherical magnetic levitation haptic interface device. In *Proceedings of the ASME Winter Annual Meeting, Symposium on Haptic Interfaces for Virtual Environment and Teleoperator Systems,(Atlanta)*.

[11] Peter J Berkelman and Ralph L Hollis. 2000. Lorentz magnetic levitation for haptic interaction: Device design, performance, and integration with physical simulations. *The International Journal of Robotics Research* 19, 7 (2000), 644–667. DOI: http://dx.doi.org/10.1177/02783649000190070 3

[12] Niloy Bhadra, P Hunter Peckham, Michael W Keith, Kevin L Kilgore, Fred Montague, Martie Gazdik, and Tom Stage. 2002. Implementation of an implantable joint-angle transducer. *Journal of rehabilitation research and development* 39, 3 (2002), 411–422.

[13] Joseph B Brink, Andrew J Petruska, David E Johnson, and Jake J Abbott. 2014. Factors affecting the design of untethered magnetic haptic interfaces. In *2014 IEEE Haptics Symposium (HAPTICS)*. IEEE, 107–114. DOI: http://dx.doi.org/doi:10.1109/HAPTICS.2014.6775441

[14] Ke-Yu Chen, Shwetak N. Patel, and Sean Keller. 2016. Finexus: Tracking Precise Motions of Multiple Fingertips Using Magnetic Sensing. In *Proceedings of the 2016 CHI Conference on Human Factors in Computing Systems (CHI '16)*. Association for Computing Machinery, New York, NY, USA, 1504–1514. DOI: http://dx.doi.org/10.1145/2858036.2858125

[15] Inrak Choi and Sean Follmer. 2016. Wolverine: A Wearable Haptic Interface for Grasping in VR. In *Proceedings of the 29th Annual Symposium on User Interface Software and Technology (UIST '16 Adjunct)*. ACM, New York, NY, USA, 117–119. DOI: http://dx.doi.org/10.1145/2984751.2985725

[16] Inrak Choi, Eyal Ofek, Hrvoje Benko, Mike Sinclair, and Christian Holz. 2018. CLAW: A Multifunctional Handheld Haptic Controller for Grasping, Touching, and Triggering in Virtual Reality. In *Proceedings of the 2018 CHI Conference on Human Factors in Computing Systems (CHI '18)*. Association for Computing Machinery, New York, NY, USA, 1–13. DOI: http://dx.doi.org/10.1145/3173574.3174228

[17] CyberGlove Systems Inc. 2017a. CyberGrasp Glove. http://www.cyberglovesystems.com/cybergrasp. (2017). Last accessed: 12.03.2017.

[18] CyberGlove Systems Inc. 2017b. CyberTouch Glove. http://www.cyberglovesystems.com/cybertouch. (2017). Last accessed: 18.03.2017.

[19] Xiaochi Gu, Yifei Zhang, Weize Sun, Yuanzhe Bian, Dao Zhou, and Per Ola Kristensson. 2016. Dexmo: An Inexpensive and Lightweight Mechanical Exoskeleton for Motion Capture and Force Feedback in VR. In *Proceedings of the 2016 CHI Conference on Human Factors in Computing Systems (CHI '16)*. ACM, New York, NY, USA, 1991–1995. DOI: http://dx.doi.org/10.1145/2858036.2858487

[20] Xinying Han, Hiroaki Seki, Yoshitsugu Kamiya, and Masatoshi Hikizu. 2007. Wearable handwriting input device using magnetic field. In *SICE Annual Conference 2007*. IEEE, 365–368. DOI: http://dx.doi.org/10.1109/SICE.2007.4421009

[21] Seongkook Heo, Christina Chung, Geehyuk Lee, and Daniel Wigdor. 2018. Thor's Hammer: An Ungrounded Force Feedback Device Utilizing Propeller-Induced Propulsive Force. In *Extended Abstracts of the 2018 CHI Conference on Human Factors in Computing Systems (CHI EA '18)*. Association for Computing Machinery, New York, NY, USA, 1–4. DOI: http://dx.doi.org/10.1145/3170427.3186544

[22] Ronan Hinchet, Velko Vechev, Herbert Shea, and Otmar Hilliges. 2018. DextrES: Wearable Haptic Feedback for Grasping in VR via a Thin Form-Factor Electrostatic Brake. In *Proceedings of the 31st Annual ACM Symposium on User Interface Software and Technology (UIST '18)*. Association for Computing Machinery, New York, NY, USA, 901–912. DOI: http://dx.doi.org/10.1145/3242587.3242657

[23] Takayuki Hoshi, Masafumi Takahashi, Takayuki Iwamoto, and Hiroyuki Shinoda. 2010. Noncontact tactile display based on radiation pressure of airborne ultrasound. *IEEE Transactions on Haptics* 3, 3 (2010), 155–165. DOI:http://dx.doi.org/10.1109/TOH.2010.4

[24] HTC. 2015. HTC Vive. (2015). https://www.vive.com/eu/.

[25] Hashim Iqbal and Byung-Ju Yi. 2019. Design and Experimental Verification of a 3-DOF Spherical Electromagnetic Brake for Haptic Interface. *International Journal of Control, Automation and Systems* (2019), 1–11. DOI: http://dx.doi.org/0.1007/s12555-019-0188-0

[26] Ali Israr and Ivan Poupyrev. 2011. Tactile Brush: Drawing on Skin with a Tactile Grid Display. In *Proceedings of the SIGCHI Conference on Human Factors in Computing Systems (CHI '11)*. Association for Computing Machinery, New York, NY, USA, 2019–2028. DOI: http://dx.doi.org/10.1145/1978942.1979235

[27] John David Jackson. 2007. *Classical electrodynamics*. John Wiley & Sons.

[28] Wendy Ju, Leonardo Bonanni, Richard Fletcher, Rebecca Hurwitz, Tilke Judd, Rehmi Post, Matthew Reynolds, and Jennifer Yoon. 2002. Origami Desk: Integrating Technological Innovation and Human-Centric Design. In *Proceedings of the 4th Conference on Designing Interactive Systems: Processes, Practices, Methods, and Techniques (DIS '02)*. Association for Computing Machinery, New York, NY, USA, 399–405. DOI: http://dx.doi.org/10.1145/778712.778770

[29] Soheil Kianzad and Karon E MacLean. 2018. Harold's purple crayon rendered in haptics: Large-stroke, handheld ballpoint force feedback. In *2018 IEEE Haptics Symposium (HAPTICS)*. IEEE, 106–111. DOI: http://dx.doi.org/10.1109/HAPTICS.2018.8357161

[30] Hwan Kim, Minhwan Kim, and Woohun Lee. 2016. HapThimble: A Wearable Haptic Device Towards Usable Virtual Touch Screen. In *Proceedings of the 2016 CHI Conference on Human Factors in Computing Systems (CHI '16)*. ACM, New York, NY, USA, 3694–3705. DOI: http://dx.doi.org/10.1145/2858036.2858196

[31] Han-Chih Kuo, Rong-Hao Liang, Long-Fei Lin, and Bing-Yu Chen. 2016. GaussMarbles: Spherical Magnetic Tangibles for Interacting with Portable Physical Constraints. In *Proceedings of the 2016 CHI Conference on Human Factors in Computing Systems (CHI '16)*. Association for Computing Machinery, New York, NY, USA, 4228–4232. DOI: http://dx.doi.org/10.1145/2858036.2858559

[32] Thomas Langerak, Juan Zarate, Velko Vechev, David Lindlbauer, Daniele Panozzo, and Otmar Hilliges. 2020. Optimal Control for Electromagnetic Haptic Guidance Systems. In *Proceedings of the 33nd Annual ACM Symposium on User Interface Software and Technology*.

[33] Thomas Langerak, Juan Zarate, Velko Vechev, Daniele Panozzo, and Otmar Hilliges. 2019. A Demonstration on Dynamic Drawing Guidance via Electromagnetic Haptic Feedback. In *The Adjunct Publication of the 32nd Annual ACM Symposium on User Interface Software and Technology (UIST '19)*. Association for Computing Machinery, New York, NY, USA, 110–112. DOI: http://dx.doi.org/10.1145/3332167.3356889

[34] Jaeyeon Lee, Mike Sinclair, Mar Gonzalez-Franco, Eyal Ofek, and Christian Holz. 2019. TORC: A Virtual Reality Controller for In-Hand High-Dexterity Finger Interaction. In *Proceedings of the 2019 CHI Conference on Human Factors in Computing Systems (CHI '19)*. Association for Computing Machinery, New York, NY, USA, Article Paper 71, 13 pages. DOI: http://dx.doi.org/10.1145/3290605.3300301

[35] WH Li, B Liu, Prabuono B Kosasih, and XZ Zhang. 2007. A 2-DOF MR actuator joystick for virtual reality applications. *Sensors and Actuators A: Physical* 137, 2 (2007), 308–320. DOI: http://dx.doi.org/10.1016/j.sna.2007.03.015

[36] Rong-Hao Liang, Kai-Yin Cheng, Chao-Huai Su, Chien-Ting Weng, Bing-Yu Chen, and De-Nian Yang. 2012. GaussSense: Attachable Stylus Sensing Using Magnetic Sensor Grid. In *Proceedings of the 25th Annual ACM Symposium on User Interface Software and Technology (UIST '12)*. Association for Computing Machinery, New York, NY, USA, 319–326. DOI: http://dx.doi.org/10.1145/2380116.2380157

[37] Thomas H. Massie and J. K. Salisbury. 1994. The PHANToM Haptic Interface: A Device for Probing Virtual Objects. In *Proceedings of the ASME Winter Annual Meeting '94 (Dynamics and Control 1994)*. 295–301.

[38] Jess McIntosh, Paul Strohmeier, Jarrod Knibbe, Sebastian Boring, and Kasper Hornbæk. 2019. Magnetips: Combining Fingertip Tracking and Haptic Feedback for Around-Device Interaction. In *Proceedings of the 2019 CHI Conference on Human Factors in Computing Systems (CHI '19)*. ACM, New York, NY, USA, Article 408, 12 pages. DOI: http://dx.doi.org/10.1145/3290605.3300638

[39] Microsoft. 2014. Xbox Official Site. (2014). https://www.xbox.com/.

[40] NeuroDigital Technologies. 2017. Gloveone Glove. https://www.neurodigital.es/gloveone/. (2017). Last accessed: 29.03.2017.

[41] Oculus. 2016. Oculus Rift. https://www.oculus.com/. (2016). Last accessed: 05.05.2020.

[42] Masa Ogata. 2018. Magneto-Haptics: Embedding Magnetic Force Feedback for Physical Interactions. In *Proceedings of the 31st Annual ACM Symposium on User Interface Software and Technology (UIST '18)*. Association for Computing Machinery, New York, NY, USA, 737–743. DOI: http://dx.doi.org/10.1145/3242587.3242615

[43] Gian Pangaro, Dan Maynes-Aminzade, and Hiroshi Ishii. 2002. The Actuated Workbench: Computer-Controlled Actuation in Tabletop Tangible Interfaces. In *Proceedings of the 15th Annual ACM Symposium on User Interface Software and Technology (UIST '02)*. Association for Computing Machinery, New York, NY, USA, 181–190. DOI: http://dx.doi.org/10.1145/571985.572011

[44] Andrew J Petruska and Jake J Abbott. 2014. Omnimagnet: An omnidirectional electromagnet for controlled dipole-field generation. *IEEE Transactions on Magnetics* 50, 7 (2014), 1–10. DOI: http://dx.doi.org/10.1109/TMAG.2014.2303784

[45] Domenico Prattichizzo, Francesco Chinello, Claudio Pacchierotti, and Monica Malvezzi. 2013. Towards Wearability in Fingertip Haptics: a 3-DoF Wearable Device for Cutaneous Force Feedback. *EEE Trans. Haptics* 6, 4 (Oct 2013), 506–516. DOI: http://dx.doi.org/10.1109/TOH.2013.53

[46] Marco Russel. 2017. *A neural network driven sensor array for locating a permanent magnet*. Master's thesis. Graduate Studies.

[47] V Schlageter, P-A Besse, RS Popovic, and P Kucera. 2001. Tracking system with five degrees of freedom using a 2D-array of Hall sensors and a permanent magnet. *Sensors and Actuators A: Physical* 92, 1-3 (2001), 37–42. DOI: http://dx.doi.org/10.1016/S0924-4247(01)00537-4

[48] Doruk Senkal and Hakan Gurocak. 2009. Spherical brake with MR fluid as multi degree of freedom actuator for haptics. *Journal of Intelligent Material Systems and Structures* 20, 18 (2009), 2149–2160. DOI: http://dx.doi.org/10.1177/1045389X09348925

[49] Doruk Senkal and Hakan Gurocak. 2011. Haptic joystick with hybrid actuator using air muscles and spherical MR-brake. *Mechatronics* 21, 6 (2011), 951–960. DOI: http://dx.doi.org/10.1016/j.mechatronics.2011.03.001

[50] Mike Sinclair, Eyal Ofek, Mar Gonzalez-Franco, and Christian Holz. 2019. CapstanCrunch: A Haptic VR Controller with User-Supplied Force Feedback. In *Proceedings of the 32nd Annual ACM Symposium on User Interface Software and Technology (UIST '19)*. Association for Computing Machinery, New York, NY, USA, 815–829. DOI: http://dx.doi.org/10.1145/3332165.3347891

[51] Richard E. Stamper. 1997. *A Three Degree Of Freedom Parallel Manipulator With Only Translational Degrees Of Freedom*. Ph.D. Dissertation. University of Maryland at College Park.

[52] S Tarantino, F Clemente, D Barone, M Controzzi, and CJSR Cipriani. 2017. The myokinetic control interface: tracking implanted magnets as a means for prosthetic control. *Scientific reports* 7, 1 (2017), 1–11. DOI: http://dx.doi.org/10.1038/s41598-017-17464-1

[53] Cameron R Taylor, Haley G Abramson, and Hugh M Herr. 2019. Low-Latency Tracking of Multiple Permanent Magnets. *IEEE Sensors Journal* 19, 23 (2019), 11458–11468. DOI: http://dx.doi.org/10.1109/JSEN.2019.2936766

[54] Bernhard Thomaszewski, Andreas Gumann, Simon Pabst, and Wolfgang Straßer. 2008. Magnets in Motion. *ACM Trans. Graph.* 27, 5, Article 162 (Dec. 2008), 9 pages. DOI:http://dx.doi.org/10.1145/1409060.1409115

[55] Valve. 2019. Valve Knuckles. (2019). https://www.valvesoftware.com/en/index/controllers.

[56] R. Q. Van Der Linde, P. Lammertse, Frederiksen E., and Ruiter B. 2002. The HapticMaster, a New Highperformance Haptic Interface. In *Proceedings of Eurohaptics 2002*.

[57] Malte Weiss, Florian Schwarz, Simon Jakubowski, and Jan Borchers. 2010. Madgets: Actuating Widgets on Interactive Tabletops. In *Proceedings of the 23nd Annual ACM Symposium on User Interface Software and Technology (UIST '10)*. Association for Computing Machinery, New York, NY, USA, 293–302. DOI: http://dx.doi.org/10.1145/1866029.1866075

[58] Malte Weiss, Chat Wacharamanotham, Simon Voelker, and Jan Borchers. 2011. FingerFlux: Near-Surface Haptic Feedback on Tabletops. In *Proceedings of the 24th Annual ACM Symposium on User Interface Software and Technology (UIST '11)*. Association for Computing Machinery, New York, NY, USA, 615–620. DOI:http://dx.doi.org/10.1145/2047196.2047277

[59] Parris Wellman and Robert D. Howe. 1995. Towards Realistic Vibrotactile Display in Virtual Environments. In *Proceedings of the ASME Dynamic Systems and Control Division*. 713–718.

[60] Junichi Yamaoka and Yasuaki Kakehi. 2013. DePENd: Augmented Handwriting System Using Ferromagnetism of a Ballpoint Pen. In *Proceedings of the 26th Annual ACM Symposium on User Interface Software and Technology (UIST '13)*. Association for Computing Machinery, New York, NY, USA, 203–210. DOI: http://dx.doi.org/10.1145/2501988.2502017

[61] Kar W Yung, Peter B Landecker, and Daniel D Villani. 1998. An analytic solution for the force between two magnetic dipoles. *Physical Separation in Science and Engineering* 9, 1 (1998), 39–52. DOI: http://dx.doi.org/10.1155/1998/79537

[62] Juan Jose Zarate, Thomas Langerak, Bernhard Thomaszewski, and Otmar Hilliges. 2020. Contact-free Nonplanar Haptics with a Spherical Electromagnet. *IEEE Haptics Symposium (HAPTICS)* (2020). DOI: http://dx.doi.org/10.1109/HAPTICS45997.2020.ras.HAP20.33.99093c10

[63] Qi Zhang, Haiwei Dong, and Abdulmotaleb El Saddik. 2016. Magnetic field control for haptic display: system design and simulation. *IEEE Access* 4 (2016), 299–311. DOI:http://dx.doi.org/10.1109/ACCESS.2016.2514978

[64] Ruisi Zhang, Andrew J Boyles, and Jake J Abbott. 2018. Six principal modes of vibrotactile display via stylus. In *2018 IEEE Haptics Symposium (HAPTICS)*. IEEE, 313–318. DOI: http://dx.doi.org/10.1109/HAPTICS.2018.8357194

[65] Clement Zheng, Jeeeun Kim, Daniel Leithinger, Mark D. Gross, and Ellen Yi-Luen Do. 2019. Mechamagnets: Designing and Fabricating Haptic and Functional Physical Inputs with Embedded Magnets. In *Proceedings of the Thirteenth International Conference on Tangible, Embedded, and Embodied Interaction (TEI '19)*. Association for Computing Machinery, New York, NY, USA, 325–334. DOI: http://dx.doi.org/10.1145/3294109.3295622

[66] Esther I Zoller, Philippe C Cattin, Azhar Zam, and Georg Rauter. 2019. Assessment of the Functional Rotational Workspace of Different Grasp Type Handles for the lambda. 6 Haptic Device. In *2019 IEEE World Haptics Conference (WHC)*. IEEE, 127–132. DOI: http://dx.doi.org/10.1109/WHC.2019.8816080